

# Improving the Filterability of Particles by Healing the Seed Particles

Lorenzo Codan,<sup>\*,†</sup> Eric Sirota,<sup>‡</sup> and Aaron Cote<sup>‡</sup>

<sup>†</sup>Crystallization Laboratory, MSD Werthenstein BioPharma GmbH, Industrie Nord 1, 6105 Schachen, Switzerland

<sup>‡</sup>Chemical Engineering Research & Development. Merck & Co., Inc., Rahway, New Jersey 07065, United States

**ABSTRACT:** A shift in particle size distribution toward smaller particle sizes has been observed in batches of Compound A Triethanolate, an isolated intermediate of a commercially available active pharmaceutical ingredient, leading to poor deliquoring of the filter cake and longer filtration times, which compromised the overall process cycle time. In the most extreme case, product breakthrough during filtration was observed, leading to significant yield loss. Compound A Triethanolate is crystallized through antisolvent addition/distillation/cooling crystallization in ethyl acetate/water/ethanol. Laboratory experiments were carried out using representative product streams in order to identify the cause for the shift in particle size distribution, which could be attributed to excessive secondary nucleation at an early stage of the process caused by the use of seed particles that have been previously dried under agitation. While statically dried particles exhibit a smooth surface, the surface of particles dried under agitation is severely damaged. Agitation during drying also leads to partial amorphization of the particles. Crystallization kinetics estimated in this work demonstrated that damaged seed particles led to an increase in the level of secondary nucleation. Analysis of historical data confirmed that the shift in particle size distribution coincided with the complete consumption of statically dried seed particles produced in pilot plant batches, thus requiring a switch in seed source to particles dried under agitation produced in manufacturing batches. As static drying is not a viable option in the production of Compound A Triethanolate because of cycle time constraints, a protocol was developed that aims at healing the seed particles to suppress secondary nucleation. Seed particles are slurried in antisolvent ethanol prior to being charged to the reactor as a slurry in order to decrease the level of amorphous content. The size of the particles produced by the subsequent crystallization increased with increasing amount of ethanol used, which can be explained by the increased capacity to dissolve amorphous content of the seed particles during healing. The increase in particle size is accompanied by reduced filter cake resistance and improved deliquoring of the filter cake. In laboratory experiments, the reduction in the filtration time achieved by using healed seed particles exceeded 1 order of magnitude.

**KEYWORDS:** *crystallization, API manufacturing, seed particle attributes, crystallization kinetics modeling*

## 1. INTRODUCTION

Multiple crystallization steps are typically implemented in the synthesis of an active pharmaceutical ingredient (API). Crystallizations of intermediate products are performed either to achieve a purity upgrade or to ease storage and shipment of intermediate products. The purity and polymorphic form of isolated intermediates are oftentimes specified, while the particle size distribution (PSD) is generally not. Although the PSD is not specified, it is desired to design the crystallization process so as to generate particles that filter and dry readily in order to limit the impact on the cycle time. This work presents a case study in which an unexpected downward shift in the particle size of an isolated intermediate during factory production led to a significant penalty in the cycle time. In the most extreme case, fine particle breakthrough during filtration was observed, leading to unacceptable yield loss.

Compound A Triethanolate is an intermediate product in the production of an API for a commercially available drug product, and its crystallization is aimed at achieving the final purity upgrade prior to the final isolation of the API. The shift in PSD led to poor deliquoring of the filter cake and longer filtration times. Analysis of historical data revealed that the shift in particle size coincided with a change in seed source. Seed particles from pilot plant batches were used in the first manufacturing batches, and after the complete consumption of

this seed source, particles of Compound A Triethanolate from previous manufacturing batches were used as seeds. It was noteworthy that the material produced in pilot plant batches had been dried without agitation while the material produced in the factory was dried in an agitated filter/dryer to reduce the drying cycle time.

Laboratory experiments using representative product streams were performed to identify the root cause for the shift in particle size. Crystallization kinetics was estimated using the commercially available software package gProms FormulatedProducts (Process Systems Enterprise Ltd., London, UK) to aid in the interpretation of the experimental results. This work presents the development of a redesigned crystallization process featuring a procedure to heal the damaged seed particles that is compliant with the current filing and affords larger particles that filter faster and thus enable reduction of the cycle time of the crystallization process to acceptable values.

## 2. MATERIALS AND METHODS

**2.1. Experimental Setup.** The majority of the crystallization experiments was performed in a 100 mL automated

Received: May 8, 2018

Published: July 20, 2018

laboratory glass reactor (EasyMax 102, Mettler-Toledo, Greifensee, Switzerland), while the two experiments aimed at determining the filterability of particles were performed in a 500 mL automated laboratory reactor (OptiMax 1001, Mettler-Toledo). Both reactors were equipped with an overhead stirrer. Pitched-blade downward impellers of different diameters with four 45° inclined blades were used. The PSD was determined offline using laser diffraction (S3500, Microtrac, Krefeld, Germany). Images of particles were taken offline using scanning electron microscopes (TM3000, Hitachi, Krefeld, Germany; Quanta 250, FEI Company, Hillsboro, OR, USA). The particles were dried in a vacuum oven (SalvisLab VC-50, Renggli, Rotkreuz, Switzerland). The solute concentrations of liquid samples were characterized by HPLC (1290 Infinity, Agilent Technologies, Basel, Switzerland). The solvent composition of liquid phases and the solvent content in solid samples were quantified by gas chromatography (7890B, Agilent Technologies). The polymorphic form of wet and dry solid samples was determined by X-ray powder diffraction (XRPD) (D8 Advance, Bruker, Karlsruhe, Germany). Particles were isolated in a Rosenmund pocket filter (De Dietrich Process Systems, Bubendorf, Switzerland) to determine the specific filter cake resistance. The weight of the filtrate during filtration was measured using a balance (PG-3001-S, Mettler-Toledo) and recorded using a custom-made application of the Labview software package (version 11.0.1, National Instruments, Austin TX, USA).

**2.2. Crystallization Process for the Isolation of Compound A Triethanolate.** Compound A Triethanolate is crystallized through a seeded crystallization in ethyl acetate/water/ethanol that includes an antisolvent addition, a distillation, and a cooling step. The current batch size is ~30 kg. Aqueous workup after the synthesis of Compound A affords a solution of Compound A dissolved in ethyl acetate containing traces of acetonitrile with a solute concentration of ~235 to 250 g of Compound A/L of solution, and 9.5 to 9.9 L of ethanol/kg of Compound A and 0.10 to 0.11 L of water/kg of Compound A are charged to the solution of Compound A followed by seeding at 39 °C with 0.4 to 0.5 wt %. Seeding is followed by aging at the same temperature over no less than 6 h. A temperature range between 30 and 42 °C is allowed at the seeding point and during the aging period. Distillation to 6.2 to 7.0 L of suspension/kg of Compound A at a temperature below 42 °C is followed by cooling to 18–28 °C. At manufacturing scale, distillation typically lasts over 10 h, while the cooldown lasts over 7 h. The agitator is operated at 105 rpm, which results in a tip speed of 1.68 m/s and power per unit volume ( $P/V$ ) inputs of 0.0112 W/L during the aging period after seeding and 0.0118 W/L after the distillation step. The particles are isolated in a filter/dryer under a positive pressure up to 28 psi using a filter cloth with a mesh size of 20  $\mu\text{m}$ . The filter cake is washed three times with ethanol after filtration: a displacement wash with 2.2 to 2.6 L of ethanol/kg of Compound A is followed by a slurry wash with 2.2 to 2.6 L of ethanol/kg of Compound A and a displacement wash with 1.4 to 1.8 L of ethanol/kg of Compound A. The filtration including the washing steps typically lasts over 15 h. The cake is agitated during drying under a nitrogen blow at temperatures below 45 °C until a loss on drying below 12 wt % is reached, which corresponds to 2.6 equiv of ethanol. The final product is thus partially desolvated Compound A Triethanolate.

All of the laboratory experiments performed at 100 mL scale were started with ~30 mL of solution consisting of Compound

A dissolved in ethyl acetate with traces of acetonitrile, while the two experiments performed at 500 mL scale were started with ~120 mL of solution. In order to ease comparison of experiments, the seeding temperature, the temperature during the subsequent aging period, and the temperature during the distillation were set to 39 °C in all of the experiments. The center point of the specified volume ranges was targeted; an isolation temperature of 18 °C was chosen. Unless otherwise specified, the particles were dried statically in the vacuum oven at 42 °C.

**2.3. Materials.** Representative product streams withdrawn from production batches prior to the addition of water and ethanol were used to perform laboratory experiments. Two batches of seed particles were used in this work: seed particles from a pilot plant batch, denoted as PPB, afforded large particles in manufacturing batches; seed particles from a manufacturing batch, denoted as MB1, yielded significantly smaller particles in manufacturing batches. Ethanol denatured with toluene, which is currently used in the manufacture of Compound A, and analytical grade ethanol (HPLC grade, Fischer Scientific UK, Loughborough, UK) were used in the crystallization experiments. Deionized water was used in all of the experiments.

### 3. POPULATION BALANCE MODELING

For a well-mixed batch reactor containing particles with a characteristic length  $L$ , the population balance equation (PBE)<sup>1</sup> can be written as

$$\frac{\partial n}{\partial t} + \frac{\partial(Gn)}{\partial L} = B - D \quad (1)$$

where  $n$  is the particle number density,  $t$  is the time,  $G$  is the growth rate, and  $B$  and  $D$  are the birth and death terms, respectively, which include agglomeration and breakage. The concentration of Compound A in solution can be obtained by solving the material balance together with the PBE:

$$\frac{dc}{dt} = -3k_v\rho_C G \int_0^\infty L^2 n \, dL \quad (2)$$

where  $k_v$  is the shape factor and  $\rho_C$  is the density of crystals. In this work, spheres have been assumed, i.e.,  $k_v = \pi/6$ . The calculated density of Compound A Triethanolate is 1.273 g/cm<sup>3</sup>.

After analysis of laboratory data, it was concluded that growth and secondary nucleation are the governing mechanisms in the course of crystallization and that agglomeration and breakage can be assumed to occur at a negligible level, i.e.,  $B = D = 0$ . An empirical size-independent power law expression (eq 3) was used to describe the crystal growth with  $k_1$ ,  $E_a$ , and  $k_2$  as fitting parameters:

$$G = k_1 e^{-E_a/RT} \left( \frac{c - c_{\text{sat}}}{\rho_{\text{mol,C}}} \right)^{k_2} \quad (3)$$

where  $c - c_{\text{sat}}$  is the difference between the actual solute concentration and the solubility and is expressed in mol/m<sup>3</sup> and  $\rho_{\text{mol,C}}$  is the molar density of the fully desolvated crystal, which is 1443 mol/m<sup>3</sup>. Secondary nucleation was assumed to be caused by crystal–impeller collisions and was described using the expression proposed by Imran et al.,<sup>2</sup> leveraging the work of Evans et al.<sup>3</sup>

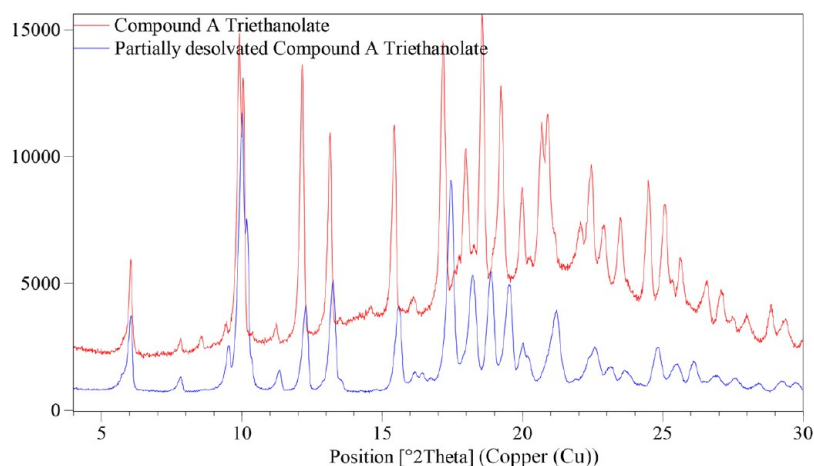


**Figure 1.** XRPD traces of wet and dry Compound A Triethanolate. The analyzed dry Compound A featured 2.1 equiv of ethanol. The halo in the XRPD trace of wet Compound A Triethanolate is caused by the Kapton film used to cover the sample in order to prevent evaporation of the solvent.

$$J_{\text{sec}} = e^{k_3}(S - 1)^{k_4} \frac{N_Q}{N_P} k_d \rho_C \varepsilon \int_{L_{\text{min}}}^{\infty} nL^3 dL \quad (4)$$

where  $k_3$ ,  $k_4$ , and  $L_{\text{min}}$  are fitting parameters;  $N_Q$  and  $N_P$  are the pumping and power number of the stirrer, respectively;  $S$  is the supersaturation, defined as the ratio between the actual concentration and the solubility; and  $\varepsilon$  is the average energy dissipation rate, defined as

$$\varepsilon = \frac{N_P d^5 n_S^3}{V} \quad (5)$$

where  $d$  is the diameter of the impeller,  $n_S$  is the stirring speed, and  $V$  is the volume of the suspension.

The initial and boundary conditions for the PBE are

$$c(0) = c_0 \quad (6)$$

$$n(0, L) = n_0 \quad (7)$$

$$n(t, 0) = \frac{J_{\text{sec}}}{G} \quad (8)$$

The mass balance and population balance equations were solved using the commercially available software gProms FormulatedProducts 1.0.2, which uses the high-resolution finite volume scheme with the flux-limiting function method (HRFVS-FL).<sup>4,5</sup> The kinetic parameters in eqs 3 and 4 were estimated by fitting a population balance model to the measured solute concentration and the measured final PSD.

#### 4. PHASE BEHAVIOR OF COMPOUND A TRIETHANOLATE

The triethanolate of Compound A is the targeted form of the crystallization process. It is the thermodynamically most stable crystal form over the entire solvent composition range covered in the course of the crystallization process and was consistently generated in laboratory experiments. Single-crystal X-ray diffraction showed that Compound A Triethanolate crystallizes in the orthorhombic crystal system with space group  $P2_12_12_1$ ,  $Z = 4$ ,  $a = 10.7355(6) \text{ \AA}$ ,  $b = 17.5150(6) \text{ \AA}$ ,  $c = 28.3142(14) \text{ \AA}$ , and  $V = 5324.0(5) \text{ \AA}^3$ . One of the ethanol molecules exhibits positional disorder and desolvates rapidly without causing a loss in crystallinity. The desolvation leads to a contraction of

the unit cell that can be detected by XRPD, as it shifts the high-angle peaks toward higher angles (Figure 1).

## 5. RESULTS AND DISCUSSION

### 5.1. Crystallization of Compound A Triethanolate at Laboratory Scale. The crystallization process for Compound

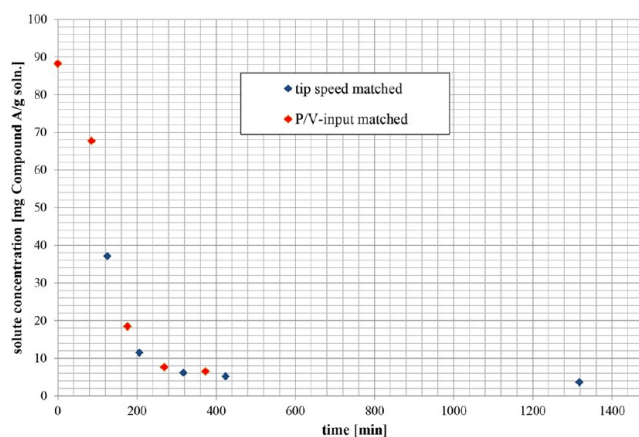


**Figure 2.** Solute concentration in the course of the aging period after seeding for the two experiments discussed in section 5.1. Seeds were introduced at time  $t = 0$ .

A Triethanolate was performed at 100 mL scale in order to assess whether the shift in particle size observed in manufacturing batches could be reproduced in the laboratory. Two different scale-down criteria were applied with the aim of assessing the mixing sensitivity of the crystallization process. In the first experiment, the agitation rate was set to approximately match the tip speed of the manufacturing process (1.68 m/s) by operating an impeller with a diameter of 3.5 cm at 800 rpm, resulting in a tip speed of 1.47 m/s. Excessive splashes were observed at higher stirring rates. In the second experiment, the approximate  $P/V$  input of the manufacturing process (0.0112 W/L) was reached by operating an impeller with a diameter of 2.5 cm at 300 rpm, resulting in a  $P/V$  input of 0.0104 W/L. Seed particles from lot MB1, which had resulted in a shift in the final PSD toward lower sizes at manufacturing scale, and analytical grade ethanol were used in both experiments. On the

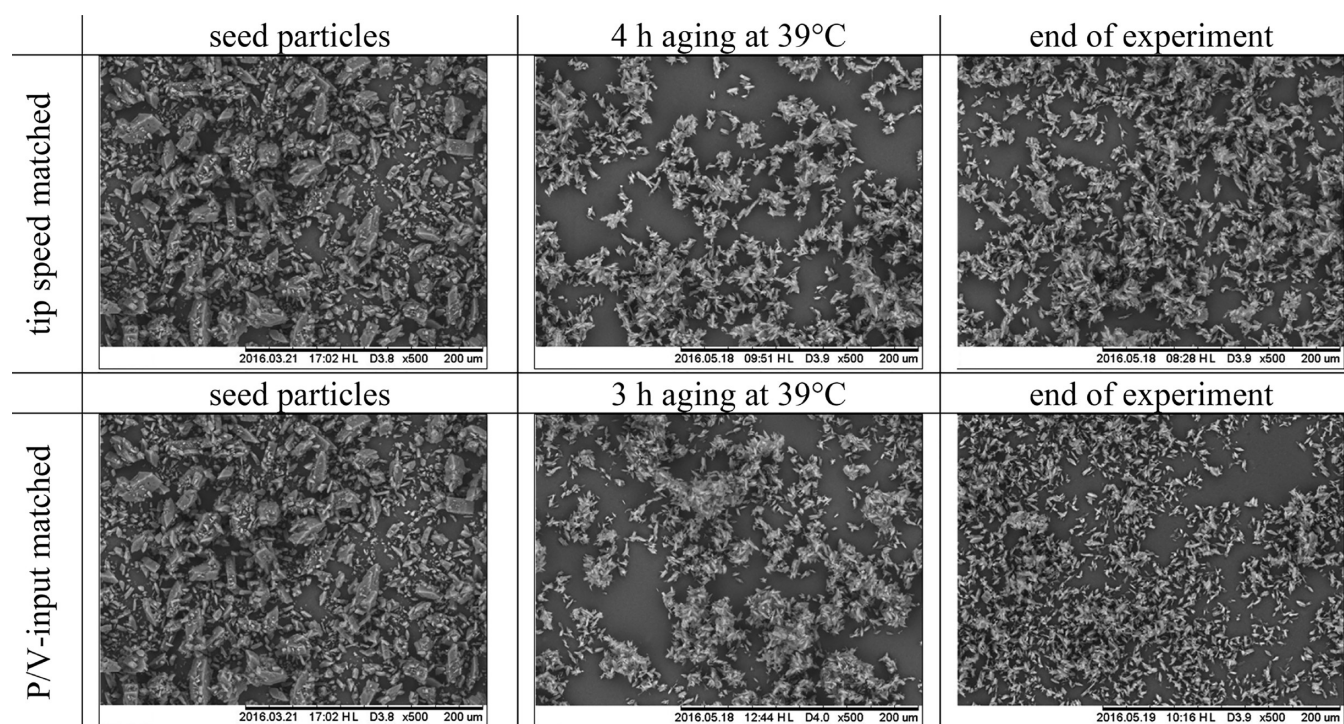


Figure 3. SEM images of particles withdrawn at different stages of the two laboratory experiments discussed in section 5.1.

**Table 1. PSDs of Particles Generated in the Two Laboratory Experiments Discussed in Section 5.1 and in the Manufacturing Plant Using Seed Particles from Lot MB1 Measured by Laser Diffraction; On the Basis of the Compact Morphology of the Particles, the Difference between the Real and Measured PSDs Is Expected to Be Small**

		mean [ $\mu\text{m}$ ]	$d_{10}$ [ $\mu\text{m}$ ]	$d_{50}$ [ $\mu\text{m}$ ]	$d_{95}$ [ $\mu\text{m}$ ]
MB1		20.72	3.94	19.26	46.54
MB2		7	2	6	17
MB3		9	3	8	21
tip-speed-matched	4 h of aging after seeding	7.43	2.05	6.39	13.49
	end of aging	6.51	2.06	5.73	11.63
	end of experiment	6.56	2.23	5.87	14.01
P/V-input-matched	3 h of aging after seeding	9.36	1.84	6.78	19.17
	end of aging	5.20	1.47	4.55	11.76
	end of experiment	5.03	1.61	4.46	10.87

**Table 2. Residual Solvent of Compound a Triethanolate Samples**

	residual ethanol		residual ethyl acetate	residual toluene
1 h in vacuum oven at 23 °C	11 wt %	2.3 equiv	0.38 wt %	ND
1 h under nitrogen blow at 23 °C	9.1 wt %	1.9 equiv	0.38 wt %	ND
PPB	8.9 wt %	1.9 equiv	0.03 wt %	ND
MB1	10.2 wt %	2.1 equiv	0.04 wt %	0.04 wt %

basis of HPLC data, almost identical solute concentration profiles were obtained in the course of the aging after seeding,

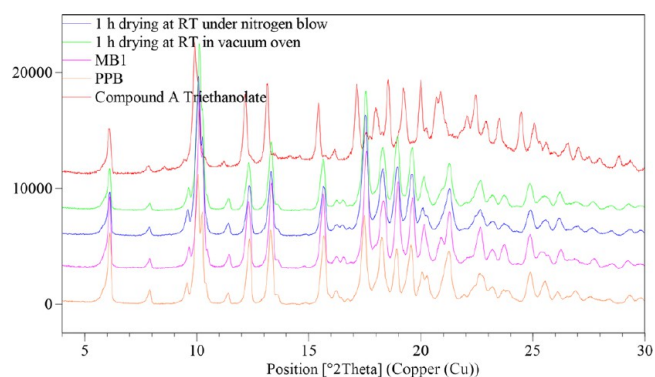


Figure 4. XRPD traces of partially desolvated Compound A Triethanolate samples compared to that of Compound A Triethanolate.

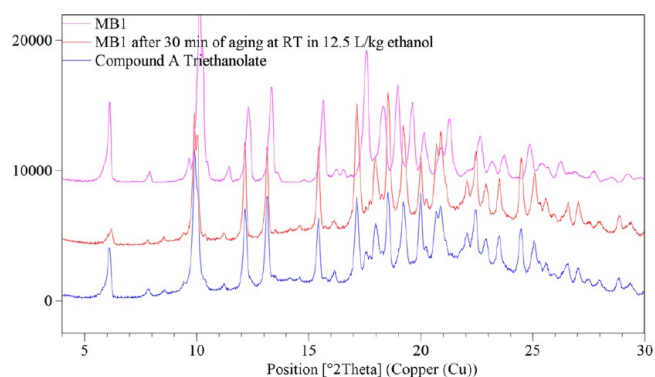
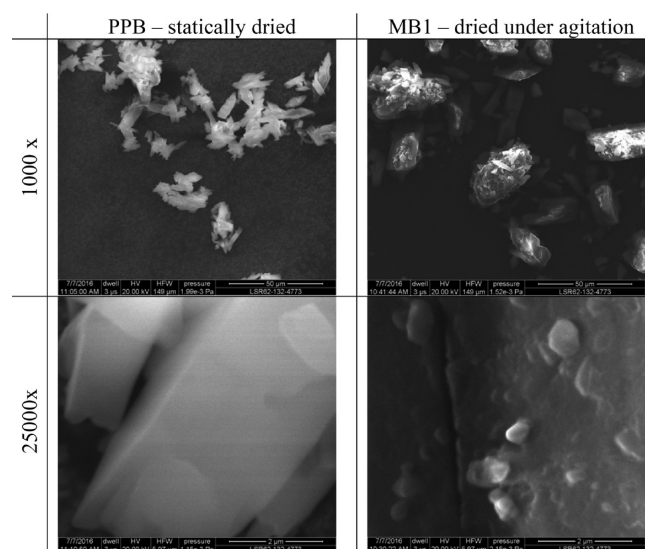
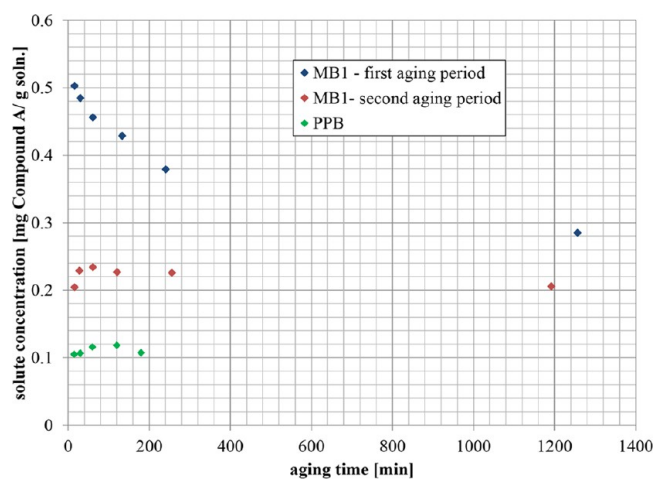


Figure 5. XRPD traces of Compound A Triethanolate particles from MB1 before and after reslurry in ethanol at 20 °C.

during which more than 90% of Compound A was crystallized (Figure 2).



**Figure 6.** SEM images of the two seed particle batches considered in this study.



**Figure 7.** Solute concentrations in the course of aging of Compound A Triethanolate seed particles in ethanol at 20 °C.

**Table 3.** Residual Solvent in the Two Batches of Seed Particles Produced To Assess the Effect of Agitation during Drying on the Final PSD

	residual ethanol		residual ethyl acetate	residual toluene
static drying	8.4 wt %	1.7 equiv	0.64 wt %	0.034 wt %
agitated drying	11 wt %	2.4 equiv	0.38 wt %	0.033 wt %

**Table 4.** PSDs of Particles Generated in the Two Laboratory Experiments Aimed at Assessing the Effect of Agitation during Drying on the Final PSD

		mean [ $\mu\text{m}$ ]	$d_{10}$ [ $\mu\text{m}$ ]	$d_{50}$ [ $\mu\text{m}$ ]	$d_{95}$ [ $\mu\text{m}$ ]
agitated drying	seed particles	13.85	5.29	12.82	27.51
	end of experiment	12.50	4.22	11.31	26.24
static drying	seed particles	21.84	12.33	19.04	37.65
	end of experiment	26.87	14.71	24.54	49.40

Scanning electron microscopy (SEM) images and PSD analyses of samples withdrawn in the course of the two experiments showed that crystallization was primarily driven by growth and secondary nucleation, and agglomeration did not appear to appreciably contribute to the final PSD (Figure 3 and Table 1).

As more than 90% of Compound A was out of solution after the extended postseeding aging period in both experiments, the outcome of this aging period was expected to have the largest impact on the PSD of the final product. In fact, the difference between the PSD of the last sample withdrawn during the aging period and the PSD of the dry product was negligibly small in both experiments. Distillation at laboratory scale lasted less than 1 h and was thus significantly faster than at manufacturing scale. However, the higher level of supersaturation reached through a faster distillation in the laboratory did not trigger late-stage secondary nucleation, as very little product was crystallizing during this operation. The shift in PSD observed at manufacturing scale could be reproduced in the laboratory, as the PSD of the particles generated in the two laboratory experiments were reasonably close to the PSDs of the particles generated in the two manufacturing batches MB2 and MB3, for which seeds from batch MB1 were used (Table 1). Slightly smaller particles were obtained when the crystallization was performed close to the  $P/V$  input of the manufacturing process, but overall, the process was relatively insensitive to agitation intensity.

**5.2. Analysis of Desolvation State across Seed Batches.** As discussed in section 4, one of the three ethanol molecules exhibits positional disorder, which leads to fast partial desolvation of Compound A Triethanolate. A series of drying experiments starting from wet Compound A Triethanolate were performed with the aim of assessing the rate of desolvation of Compound A Triethanolate. Approximately 1 equiv of ethanol was removed from the crystal lattice within an hour of drying in the vacuum oven at temperatures equal to or above 23 °C (Table 2). Similar drying behavior was observed when the particles were dried under a nitrogen blow at room temperature. In both cases, a contraction of the unit cell was detected by XRPD (Figure 4). On the basis of the outcome of the drying experiments, it is very unlikely to avoid desolvation and thus preserve the Compound A Triethanolate form over the drying process. In line with the results generated in the laboratory, the seed particles of the two manufacturing batches considered in this study were in a partially desolvated state, had comparable levels of residual solvent, and also had similar XRPD traces (Table 2 and Figure 4). The subtle differences between the XRPD traces of particles from PPB and MB1 may be attributed to different levels of desolvation.

Once desolvated, the triethanolate form can be readily re-established by reslurrying the particles in ethanol, i.e., the antisolvent used in the current crystallization process. Irrespective of the purity of ethanol used (absolute vs denatured), Compound A Triethanolate was obtained from partially desolvated powder within 30 min of aging in 12.5 L of ethanol/kg of API at 20 °C (Figure 5). Hence, partially desolvated seed particles are expected to rapidly resolvate when introduced into the batch and become active seed particles. Since the differences in residual solvent and crystal form between the two manufacturing batches MB1 and PPB are small and that resolution to Compound A Triethanolate is rapid, it can be reasonably concluded that differences in the level of desolvation across batches of seed were not the cause

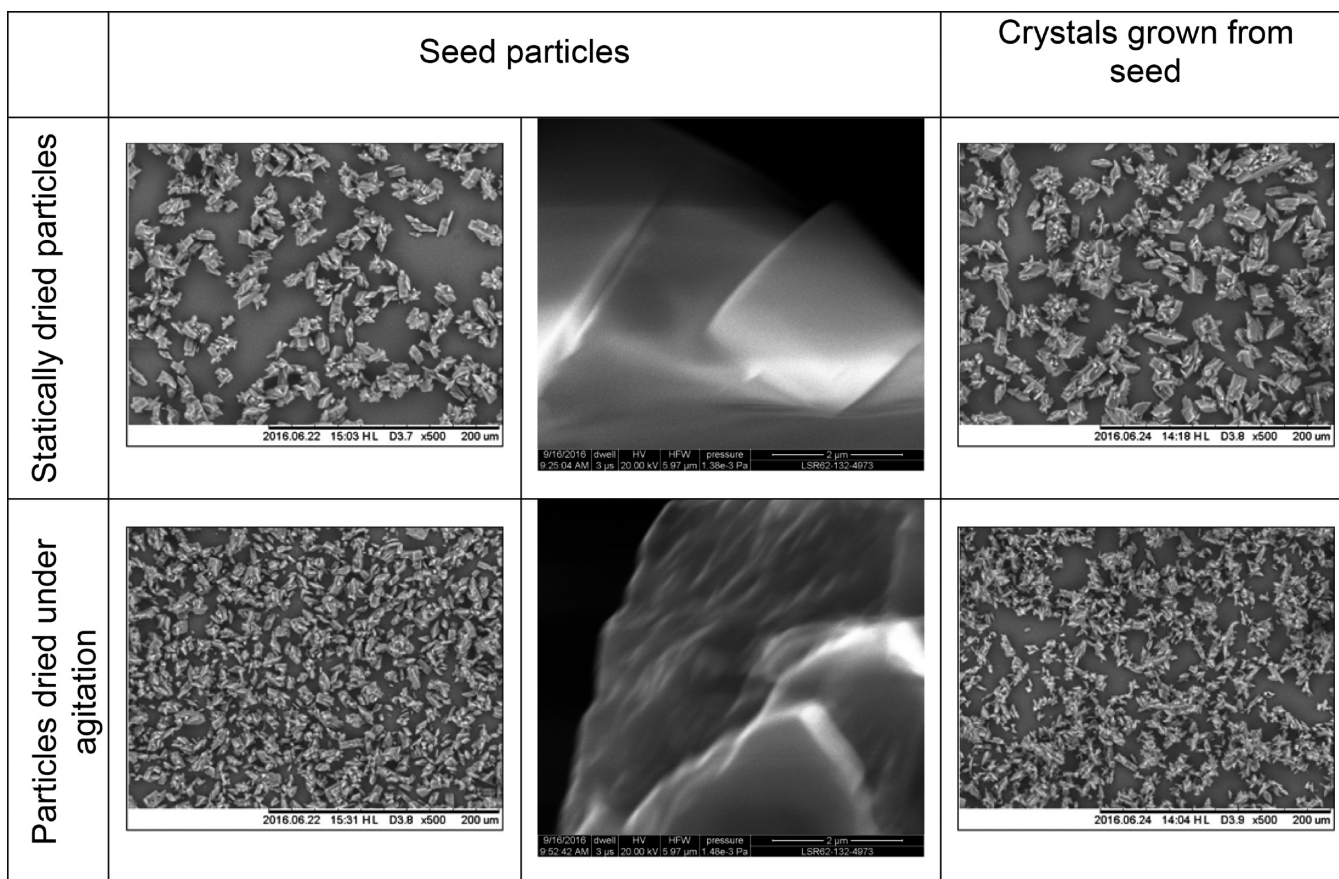


**Figure 8.** SEM images of the seed particles and the final product of the laboratory experiments discussed in section 5.4. The left column refers to the experiment in which seed particles dried statically in the laboratory were used; the right column refers to the experiment in which seed particles dried under agitation in the laboratory were used.

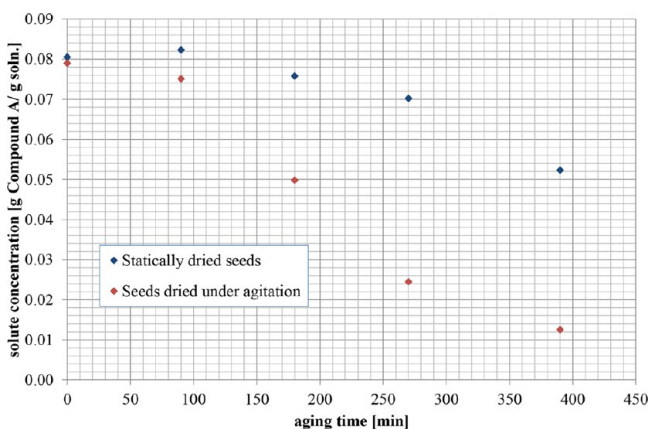


**Figure 9.** Effect of seed particle quality on the desupersaturation after seeding.

for the shift in PSD. If anything, one might have expected MB1 to be the more readily active seed, as its ethanol content was higher than that of PPB.

**5.3. Analysis of the Drying Protocol Applied for the Seed Particles.** After the state of desolvation was ruled out as the cause of the shift in particle size distribution, the focus was set to the protocol applied to dry the seed particles. Compound A Triethanolate produced in pilot plant batches was dried statically under a nitrogen blow, while because of the increased size of the batch, agitation had to be applied in

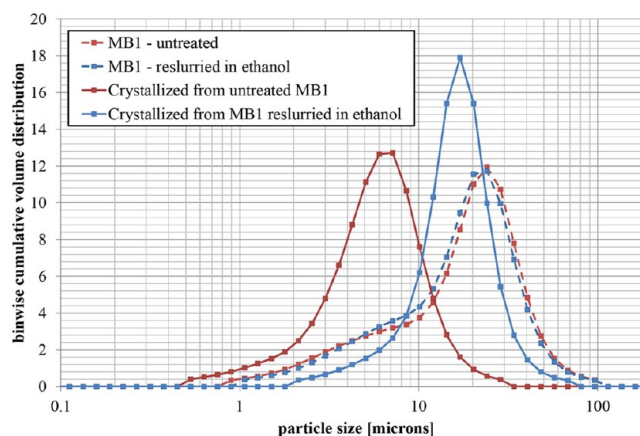


**Figure 10.** Effect of reslurrying particles in ethanol prior to their charge in the reactor on the PSDs of the seed particles and the final product.

manufacturing batches to accelerate removal of solvent while drying under a nitrogen blow. It thus had to be assessed whether agitation during drying had an impact on the particle properties and their crystallization kinetics. High-resolution SEM images showed that agitation severely damaged the particles' surface (Figure 6). The surface of the statically dried particles was smooth, while the surface of particles dried under agitation was rough.

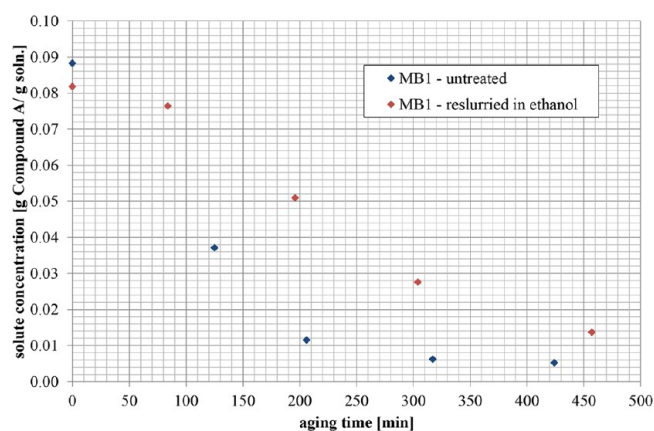


**Figure 11.** Effect of reslurrying seed particles in ethanol prior to their charge in the reactor on the desupersaturation profile during the aging after seeding.

It also had to be assessed whether surface roughening was accompanied by a loss in crystallinity. The difference in solubility between the amorphous and crystalline materials was leveraged to qualitatively assess the difference in amorphous content between the two seed batches. As Compound A Triethanolate is the most stable/least soluble form in ethanol, if the powder featured an amorphous content, the solute concentration in the course of aging in neat ethanol would peak at values above the solubility of Compound A Triethanolate, which was measured to be 0.09 mg of Compound A/g of solution. The dissolved amount of Compound A would subsequently recrystallize as Compound A Triethanolate, and the solute concentration would approach the solubility of Compound A Triethanolate. Particles from the seed batches PPB and MB1 were reslurried in 50 L of ethanol/g of Compound A Triethanolate at 20 °C. Supernatant samples were periodically withdrawn in the course of the aging period and analyzed by HPLC. In both cases, a maximum in the solute concentration was reached in the course of aging (Figure 7). However, the solute concentration peaked at a significantly higher level when reslurrying particles from MB1, which were previously dried under agitation. This outcome indicated that particles dried under agitation featured a higher level of amorphous content than those dried statically. As XRPD analysis of particles from batch MB1 did not indicate an appreciable loss in crystallinity (Figure 4), the amorphization of the particles is most likely limited to the outer layer of the particles, which was exposed to high shear during agitated drying. After drying of the reslurried particles from MB1 to approximately 2 equiv of ethanol under static conditions to prevent further damage to the particles' surface, the particles were reslurried for a second time in neat ethanol. The solute concentration peaked at significantly lower levels during the second reslurry period, thus indicating that the initial

reslurrying had enabled at least a partial digestion of the particle surface disorder and increased the particle crystallinity. This also showed that the peak in solubility was not due merely to the partial desolvation of the triethanolate.

**5.4. Confirmation of the Negative Impact of Agitation during Drying.** Analysis of the seed particles showed that the drying protocol applied at manufacturing scale led to significant damage to and partial amorphization of the particles' surface. Laboratory experiments were performed with the aim of confirming that the damage caused by agitation was the reason for the reduction in particle size in crystallizations using these seeds. The current crystallization process was run at 100 mL scale to prepare seed particles dried under different conditions. After filtration and washing, the filter cake was split in two portions. One portion was dried in the vacuum oven at 42 °C over 50 min; the other portion was dried in the EasyMax reactor over 40 min, whereby the jacket temperature was set to 42 °C and agitation was provided by a large magnetic stirring bar to simulate conditions of high shear in an industrial filter/dryer. In line with previous experiments, desolvation to approximately 2 equiv of ethanol occurred irrespective of the drying protocol (Table 3). Moreover, the statically dried particles exhibited a lower residual solvent level than those dried under agitation. As the same trend was also observed for particles dried at larger scale, it is hypothesized that the amorphization caused by agitation inhibits solvent removal. Agitation during drying led to a reduction in particle size and also to damage of the particles' surface (Table 4 and Figure 8).

The two populations of particles were used as seeds in two laboratory experiments run at 100 mL scale at a tip speed close to the one at manufacturing scale. The outcomes of the two crystallization experiments were markedly different, as significantly smaller particles were obtained when seed particles dried under agitation were used (Figure 8 and Table 4). HPLC analysis of samples withdrawn during the postseeding aging period showed that the desupersaturation was faster when seed particles previously dried under agitation were used (Figure 9). As the PSDs of the seed particles in the two experiments were different, the modeling exercise described in section 5.6 was required to assess the impact of the seed preparation on the crystallization kinetics.

**5.5. Effect of Reslurrying the Particles in Ethanol To Digest Amorphous Content.** On the basis of the results discussed in section 5.3, the damage caused by agitated drying is accompanied by partial amorphization of the particles' surface, and reslurrying the seed particles in ethanol enabled at least partial digestion of the amorphous content. After analysis of regulatory documentation, it was concluded that reslurrying the seed in ethanol prior to charging it to the reactor is compliant with the filed process. A laboratory experiment was performed in which seed particles from MB1 were used after reslurrying in 12 L of ethanol/kg of powder at 20 °C for 3 days

**Table 5. Kinetic Parameters of Equations 3 and 4 Describing Growth and Secondary Nucleation, Respectively, for Four Different Batches of Seed Particles**

	untreated MB1	MB1 reslurried in ethanol	seed particles dried under agitation in the laboratory	statically dried seed particles
$k_1$ [m/s]	$1.32 \times 10^{-7}$	$2.16 \times 10^{-7}$	$2.31 \times 10^{-7}$	$2.38 \times 10^{-7}$
$k_2$	1.62	1.69	1.76	1.84
$k_3$ [log(1/J)]	20.08	15.28	15.84	15.19
$k_4$	1.72	1.83	2.26	1.75
$L_{\min}$ [ $\mu\text{m}$ ]	0.55	1.02	2.36	9.77

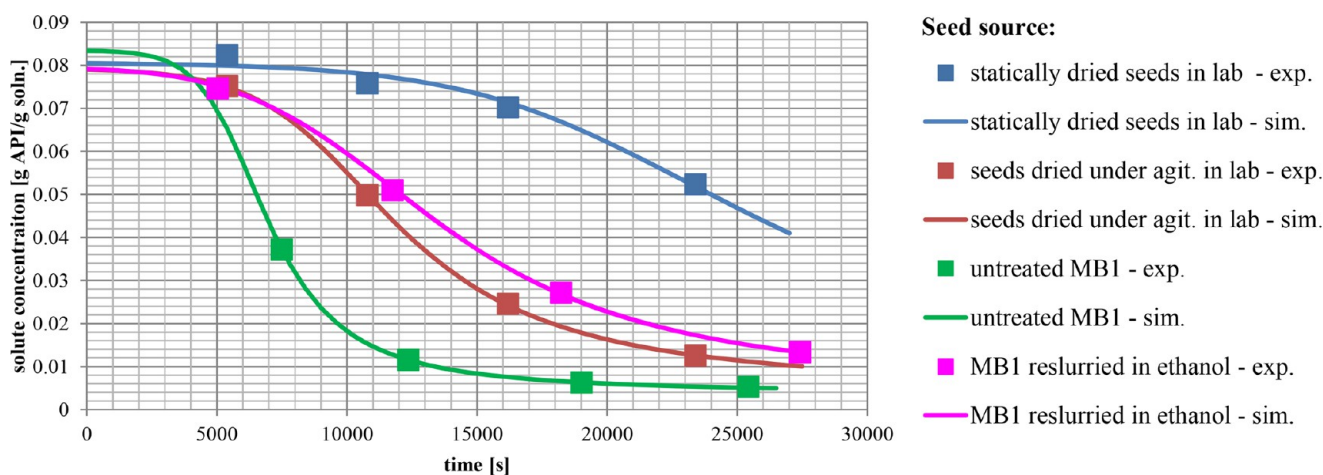


Figure 12. Measured vs simulated solute concentrations for the four experiments used to estimate the kinetic parameters. Seeding occurred at  $t = 0$ .

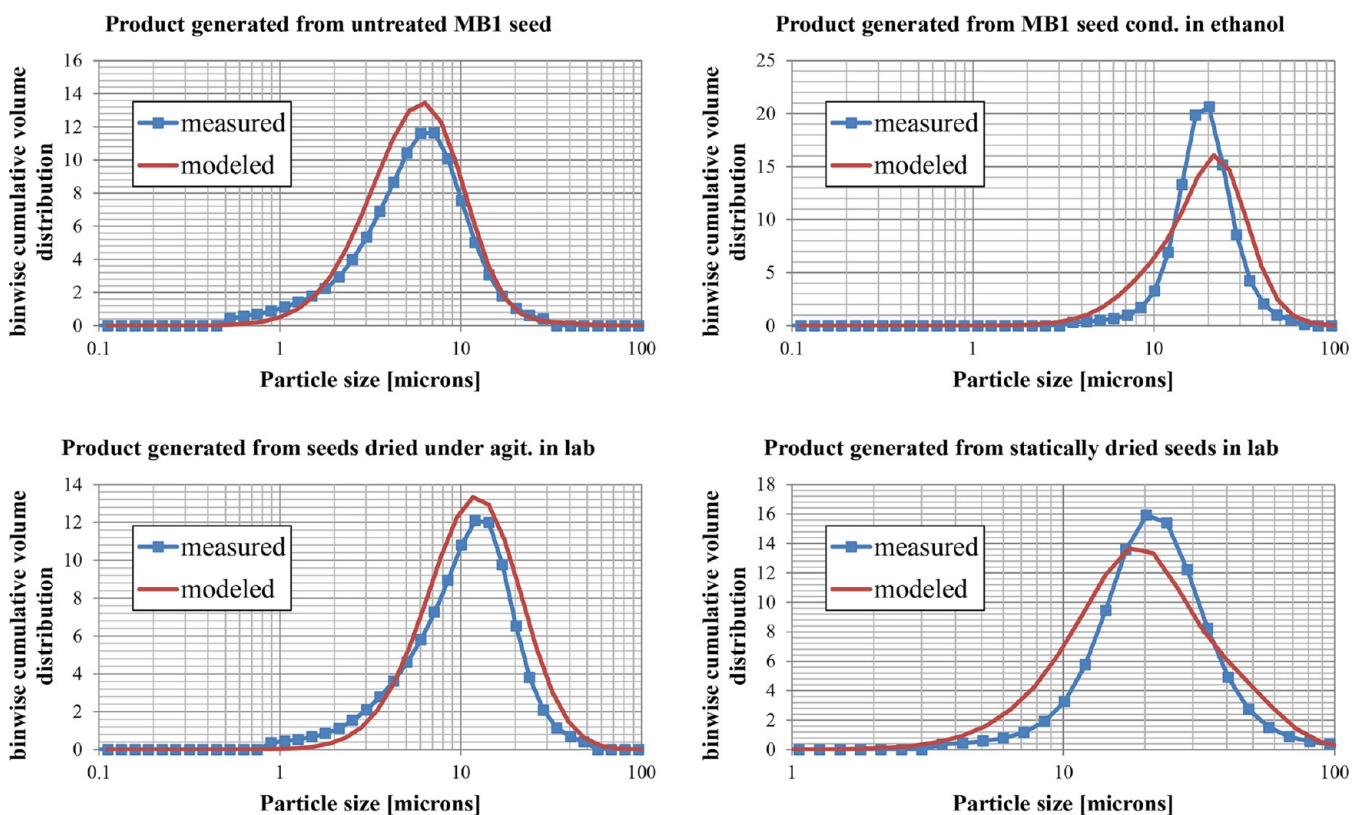
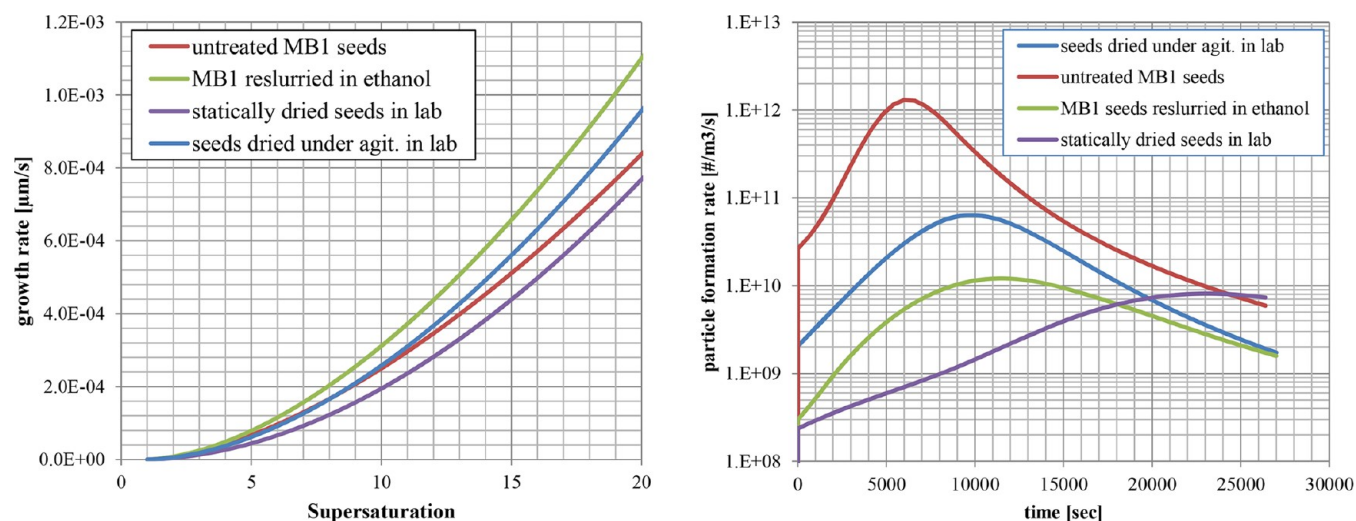


Figure 13. Measured vs simulated final PSDs of the four experiments used to estimate the kinetic parameters for different seed sources.

in order to assess whether pretreatment of the seed particles leads to a favorable change in the crystallization kinetics and an increase in particle size at the end of crystallization. The shift in the PSD of the seed particles during the aging period in ethanol was minimal (Figure 10), but partial digestion of the amorphous content enabled a shift in the PSD of the isolated product toward larger sizes. The desupersaturation was slower compared with the desupersaturation obtained when untreated seed particles were used (Figure 11). The experiment was repeated using ethanol denatured with toluene, which is currently used in the manufacture of Compound A. As an almost identical solute concentration profile and final PSD were obtained, the presence of toluene is expected to have a negligible effect on the outcome of the crystallization. Hence,

reslurrying the particles in ethanol and charging the seed as a slurry rather than a dry solid is an effective and compliant option to shift the final PSD toward larger sizes. As with the experiments presented in section 5.4, a modeling exercise was required to assess the effect of the proposed seed conditioning on the crystallization kinetics.

**5.6. Estimation of Crystallization Parameters.** The damage to the seed particles caused by agitated drying was found to alter the crystallization kinetics. Reslurrying the seed particles in ethanol before charging to the reactor was found to at least partially digest the amorphous content and to enable an increase in the size of the resulting product crystals. Kinetic parameters were estimated in order to enable deconvoluted interpretation of the results obtained in the laboratory



**Figure 14.** Calculated growth rates as functions of supersaturation and rates of particle formation in the course of aging after seeding for the four batches with different seed sources.

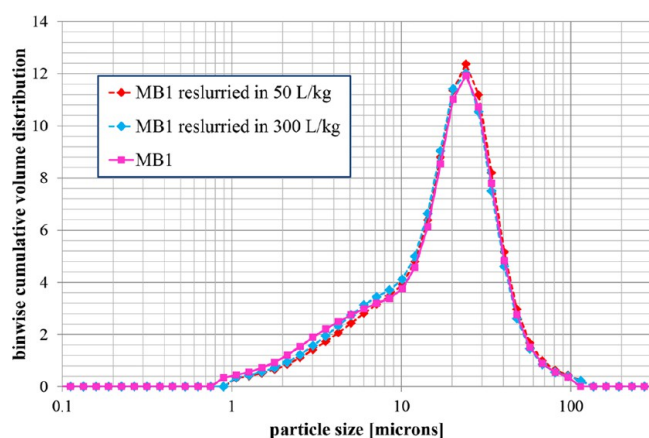


**Figure 15.** Effect of reslurrying the particles in ethanol on the PSD.

**Table 6.** Effect of the Amount of Ethanol Used To Reslurry the Seed Particles on the Final Product PSD

ethanol volume	mean [ $\mu\text{m}$ ]	$d_{10}$ [ $\mu\text{m}$ ]	$d_{50}$ [ $\mu\text{m}$ ]	$d_{95}$ [ $\mu\text{m}$ ]
dry seed particles	20.7	3.94	19.3	46.6
0 L/kg	6.97	2.44	6.34	14.5
20 L/kg	16.2	8.00	15.0	30.1
50 L/kg	18.8	10.4	17.5	33.9
100 L/kg	20.1	11.5	18.7	35.7
200 L/kg	23.0	13.9	21.4	39.6
300 L/kg	27.6	17.4	25.6	46.4

experiments. As the outcome of the crystallization process was found to be strongly dependent on the properties of the seed particles, the growth and secondary nucleation kinetics were expected to vary across batches of seed. Hence, a set of growth and secondary nucleation parameters was estimated for each population of seed particles. Model parameters were estimated for the untreated seed particles from batch MB1 using the experimental data of section 5.1, for the seed particles from MBI reslurried in ethanol using the experimental data of section 5.5, and for the two seed population batches produced in the laboratory using the experimental data of section 5.4. Only the isothermal aging period after seeding was considered for the parameter fitting exercise because this is where 90% of

the crystallization occurs (i.e., the crystallization during distillation and subsequent cooling was not incorporated into this analysis). The activation energy  $E_a$  could thus be set to 0 for this regression. As only  $\sim 2$  wt % of the total amount of ethanol is incorporated in the crystals during the aging time after seeding, the solvent composition of the liquid was assumed to be constant over the entire aging period, and the density of the liquid phase was estimated using data reported by Pires et al.<sup>6</sup> The values of 1.3 and 0.79 proposed by the gProms FormulatedProduct software were taken for the power and the pumping number, respectively. The solute concentration profile and the PSD of the dry product were used to estimate the kinetic parameters describing growth and secondary nucleation. Table 5 shows the five model parameters estimated for each population of seed particles; Figures 12 and 13 show the experimental and simulated solute concentration and PSD data, respectively. The model is able to describe the outcome of the experiment reasonably well. In order to compare the growth and secondary nucleation kinetics across seed particle batches, Figure 14 shows the growth rate as a function of supersaturation for the four different seed particle populations and the simulated rate of particle formation as a function of time for the four different seed particle populations. While similar growth rates were obtained for the four different seed particle batches, the opposite is true for the rate of secondary nucleation. The highest secondary nucleation rate was obtained for seed particles previously dried under agitation in the factory. Hence, the damage caused by agitation was found to trigger secondary nucleation, and this dominance of secondary nucleation explains the more rapid relief of supersaturation for these batches and the downward shift in particle size. The level of damage reached in the laboratory experiment was lower than the one obtained at manufacturing scale, as the modeling exercise revealed lower rates of secondary nucleation. Reslurrying MBI particles before they were charged to the reactor resulted in decreased rates of secondary nucleation. Hence, the partial digestion of the amorphous content achieved by reslurrying the particles in ethanol led to partial suppression of secondary nucleation, which explains the increased particle size of the resulting product.

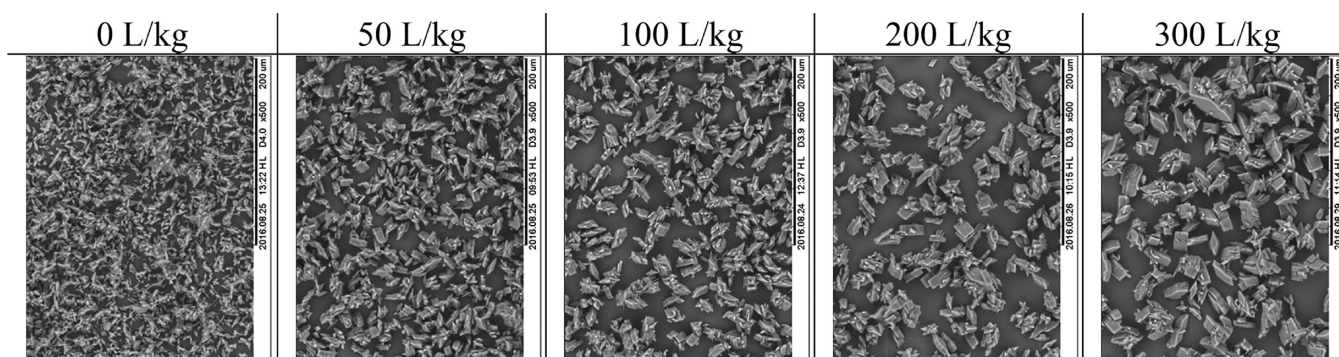


**Figure 16.** Effect of the amount of ethanol used to reslurry the seed particles over ~16 h at 20 °C on the final PSD.

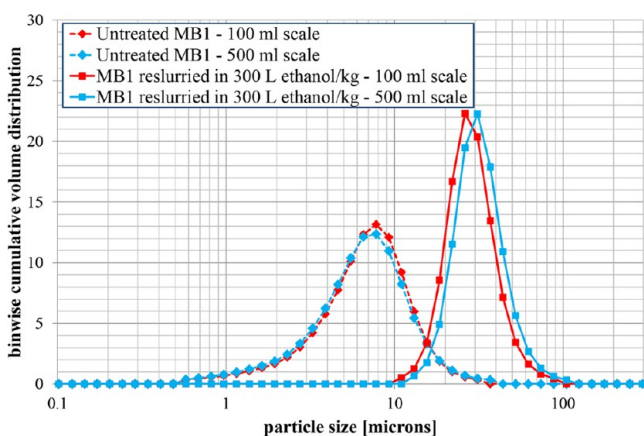


**Figure 17.** Comparison of final PSDs obtained in experiments performed at 100 and 500 mL scale.

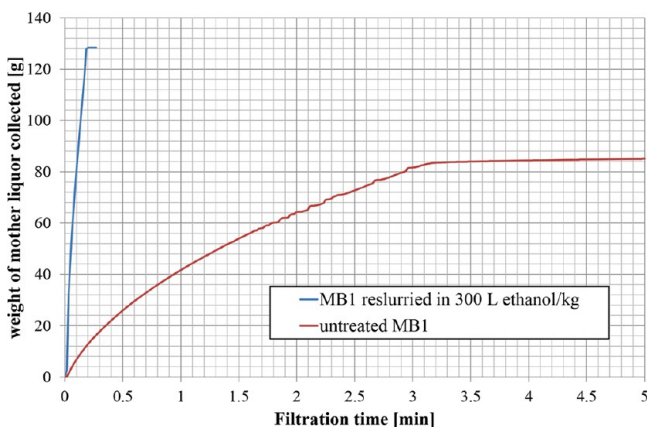


**Figure 18.** Weight of filtrate collected in the course of the filtration experiments performed to determine the specific cake resistance.

**5.7. Development of a Remediation Plan.** After the root cause for the decrease in particle size had been identified, a remediation plan had to be established in order to increase the particle size. Static drying is not a suitable option, as it would result in excessively long drying times and inhomogeneous levels of residual solvent in the cake. As the reslurry period aimed at partially digesting the amorphous content created during agitated drying involves partial dissolution and recrystallization, its efficacy in healing the particles' surface is expected to depend on the amount of solvent used, the aging temperature, and the aging time. In order to ease implementation in the manufacturing plant, the aging time

was fixed at 16 h, i.e., the equivalent of an overnight age, and the aging temperature was set at 20 °C. The conditions chosen would allow the reslurry period to be performed in a blow can equipped with an overhead stirrer. After scrutiny of the available equipment, the maximal amount of ethanol that could be used to reslurry the particles was 350 L of ethanol/kg of powder, i.e. ~1.5 L of ethanol/kg with respect to the total amount of Compound A being crystallized. A series of experiments was conducted with the aim of assessing the effect on final product PSD of varying the amount of ethanol used to condition the seeds. The volume chosen to reslurry the seed particles ranged from 20 to 300 L of ethanol/kg of seeds. Ethanol denatured with toluene was used in all of the experiments to align with the solvent used in the commercial process. On the basis of HPLC data, the mass of dissolved particles at the end of aging never exceeded 8%. In agreement with the results presented in section 5.5, reslurrying the particles in ethanol led to a negligible change in PSD, as shown in Figure 15 for a subset of the experiments. After overnight aging in ethanol, the seed particles were charged as a slurry to a series of identical crystallizations. The amount of ethanol charged to the reactor was adjusted to keep the initial concentration the same in all of the experiments. The tip speed during crystallization was set so as to match the tip speed applied in the manufacturing process. In line with expectations, the final PSD shifted toward larger particle sizes as more ethanol was used to reslurry the seed particles (Table 6 and Figure 16). The final particle size increased with increasing amount of ethanol used and did not level off in the range tested. When ethanol volumes equal to or larger than 100 L of ethanol/kg of powder were used, the average diameter of the product particles was equal to or larger than the average diameter of the seed particles.

**5.8. Assessment of Filterability.** The increase in particle size achieved by reslurrying the seed particles in ethanol is also expected to benefit the filterability of particles. Two crystallization processes were conducted in an Optimax 500 mL reactor with the aim of producing enough Compound A Triethanolate to enable isolation in a pressure pocket filter. In the first experiment, untreated seed particles from batch MB1 were used, while in the second experiment the seed particles were reslurried in 300 L of ethanol/kg of powder prior to being charged to the reactor. Similar PSDs were obtained compared to the experiments run at 100 mL scale under the same conditions (Figure 17).

The particles were isolated at ~12 psi using a pressure filter. The filtrate weight was monitored over time (Figure 18) to

estimate the specific filter cake resistance  $\alpha$  by assuming an incompressible cake and using eq 9:<sup>7</sup>

$$\frac{\Delta P A t}{\mu V_F} = \alpha \left( \frac{WV}{2A} \right) + R_m \quad (9)$$

where  $\Delta P$  is the pressure,  $A$  is the area of the filter,  $\mu$  is the viscosity of the filtrate,  $V_F$  is the volume of the filtrate,  $W$  is the suspension density, and  $R_m$  is the medium resistance. The filter diameter was 49.5 mm. The final solvent composition in both experiments was 95 mol % ethanol and 5 mol % ethyl acetate, which according to Gonzales et al.<sup>8</sup> results in a viscosity of 1.05 cP and a density of 0.798 g/mL under the assumption that Compound A has a negligible impact on the viscosity and density; the suspension density at the end of the experiment was  $\sim 180$  g of Compound A Triethanolate/L of solution.  $\alpha$  and  $R_m$  were estimated by fitting eq 9 to experimental data.

The use of untreated seed particles afforded particles with a specific filter cake resistance of  $5.8 \times 10^{10}$  m/kg, which classifies the particles as slow filtering.<sup>7</sup> As filter breakthrough was observed at laboratory scale, the particles generated from untreated seed particles of batch MB1 had to be filtered using a 0.2  $\mu\text{m}$  nylon filter. The specific filter cake resistance of particles generated from the seed particles reslurried in 300 L of ethanol/kg of powder was  $9.3 \times 10^8$  m/kg, which classifies the particles as moderately fast filtering.<sup>7</sup> The decrease in the specific filter cake resistance translates to an  $\sim 60$ -fold reduction in the filtration time. In addition, on the basis of the collected mass of filtrate, the deliquoring of particles crystallized from pretreated seed particles is significantly more efficient, leaving the resulting cake with a much lower residual solvent level.

## 6. CONCLUSIONS

This work provides insights into the importance of the quality of the seed particles in crystallization processes as previously highlighted by Aamir et al.<sup>9</sup> The implementation of agitation to facilitate drying of an intermediate product was found to cause significant damage and partial amorphization of the particles. Although not critical for the release of the intermediate, the damage caused by agitated drying was also found to inhibit removal of solvent. When used as seeds, the damaged, partially amorphous particles resulted in a significant shift in the PSD of the crystallized intermediate toward smaller particles, leading to a penalty in the filtration performance. Estimation of the crystallization kinetics showed that the use of damaged seed particles led to an increased level of secondary nucleation compared with the use of statically dried seed particles. As static drying is not a viable option at manufacturing scale, a protocol was developed that is compliant with the current filing and achieves partial digestion of the amorphous content by reslurrying the seed particles in ethanol overnight at 20 °C. Laboratory experiments confirmed that the developed protocol results in an increase in the final particle size of the product and improves the filterability of the particles.

## AUTHOR INFORMATION

### Corresponding Author

\*E-mail: [lorenzo.codan@merck.com](mailto:lorenzo.codan@merck.com).

### ORCID

Lorenzo Codan: 0000-0001-5654-7345

### Notes

The authors declare no competing financial interest.

## ACKNOWLEDGMENTS

We acknowledge Shelly Long and Eamon Joyce for providing representative product streams, Andrew Brunskill for scientific discussions, and Marc Grynbaum and Erdal Yavavli for analytical support.

## ABBREVIATIONS

$A$	area of pressure filter [ $\text{m}^2$ ]
$B$	birth term in PBE [ $\text{m}^{-4} \text{s}^{-1}$ ]
$c$	concentration of Compound A [kg of Compound A/ $\text{m}^3$ of solution]
$c_0$	concentration of Compound A at seeding point [kg of Compound A/ $\text{m}^3$ of solution]
$c_{\text{sat}}$	solubility of Compound A [kg of Compound A/ $\text{m}^3$ of solution]
$d$	diameter of the impeller [m]
$D$	death term in PBE [ $\text{m}^{-4} \text{s}^{-1}$ ]
$E_a$	activation energy [J/mol]
$G$	growth rate [m/s]
$J_{\text{sec}}$	secondary nucleation rate [ $\text{m}^{-3} \text{s}^{-1}$ ]
$k_v$	volume shape factor
$L$	characteristic particle length [m]
$N_P$	impeller power number
$N_Q$	impeller pumping number
$N$	particle size distribution [ $\text{m}^{-4}$ ]
$n_0$	particle size distribution of seed particles [ $\text{m}^{-4}$ ]
$n_s$	stirring speed [rps]
$R_m$	medium resistance [ $\text{m}^{-1}$ ]
$S$	supersaturation
$t$	time [s]
$V$	volume of suspension [ $\text{m}^3$ ]
$V_F$	volume of filtrate [ $\text{m}^3$ ]
$W$	suspension density [kg/L]
$\Delta P$	filtration pressure [psi]
$\alpha$	specific filter cake resistance [ $\text{m}/\text{kg}^1$ ]
$\epsilon$	average energy dissipation rate [ $\text{m}^2/\text{s}^3$ ]
$\rho_C$	density of crystals [ $\text{g}/\text{cm}^3$ ]
$\rho_{\text{mol},c}$	molar density of crystals [ $\text{mol}/\text{m}^3$ ]
$\mu$	viscosity [cP]

## REFERENCES

- (1) Randolph, A.; Larson, M. A. *Theory of Particulate Processes*; Academic Press: San Diego, CA, 1988.
- (2) Imran, A.; Wolf, E.; Kramer, H. J. M.; Jansens, P. J. Contribution of crystal–impeller and crystal–crystal collisions to secondary nucleation. Presented at the European Congress of Chemical Engineering (ECCE-6), Copenhagen, Sept 16–20, 2007.
- (3) Evans, T. W.; Sarofim, A. F.; Margolis, G. Models of Secondary Nucleation Attributable to Crystal–Crystallizer and Crystal–Crystal Collisions. *AIChE J.* **1974**, *20* (5), 959–966.
- (4) Qamar, S.; Warnecke, G. Numerical solution of population balance equation for nucleation, growth and aggregation processes. *Comput. Chem. Eng.* **2007**, *31* (12), 1576–1589.
- (5) Qamar, S.; Warnecke, G.; Elsner, M. P. On the solution of population balance equation for nucleation, growth, aggregation and breakage processes. *Chem. Eng. Sci.* **2009**, *64* (9), 2088–2095.
- (6) Pires, R. M.; Costa, H. F.; Ferreira, A. G. M.; Fonseca, I. M. A. Viscosity and Density of Water + Ethyl Acetate + Ethanol Mixtures at 298.15 and 318.15 K and Atmospheric Pressure. *J. Chem. Eng. Data* **2007**, *52*, 1240–1245.
- (7) Murugesan, S.; Hallow, D. M.; Vernille, J. P.; Tom, J. W.; Tabora, J. E. Lean Filtration: Approaches for the Estimation of Cake Properties. *Org. Process Res. Dev.* **2012**, *16*, 42–48.

(8) González, B.; Calvar, N.; Gómez, E.; Domínguez, A. Density, dynamic viscosity, and derived properties of binary mixtures of methanol or ethanol with water, ethyl acetate, and methyl acetate at  $T = (293.15, 298.15, \text{ and } 303.15) \text{ K}$ . *J. Chem. Thermodyn.* **2007**, *39*, 1578–1588.

(9) Aamir, E.; Nagy, Z. K.; Rielly, C. D. Evaluation of the Effect of Seed Preparation Method on the Product Crystal Size Distribution for Batch Cooling Crystallization Processes. *Cryst. Growth Des.* **2010**, *10*, 4728–4740.